Transient anchorage of cross-linked glycosyl-phosphatidylinositol–anchored proteins depends on cholesterol, Src family kinases, caveolin, and phosphoinositides

Yun Chen,[1,3] William R. Thelin,[1] Bing Yang,[1] Sharon L. Milgram,[1] and Ken Jacobson[1,2]

[1]Department of Cell and Developmental Biology, [2]Lineberger Comprehensive Cancer Center, and [3]Department of Biomedical Engineering, University of North Carolina School of Medicine, Chapel Hill, NC 27599

How outer leaflet plasma membrane components, including glycosyl-phosphatidylinositol–anchored proteins (GPIAPs), transmit signals to the cell interior is an open question in membrane biology. By deliberately cross-linking several GPIAPs under antibody-conjugated 40-nm gold particles, transient anchorage of the gold particle–induced clusters of both Thy-1 and CD73, a 5′ exonucleotidase, occurred for periods ranging from 300 ms to 10 s in fibroblasts. Transient anchorage was abolished by cholesterol depletion, addition of the Src family kinase (SFK) inhibitor PP2, or in Src-Yes-Fyn knockout cells. Caveolin-1 knockout cells exhibited a reduced transient anchorage time, suggesting the partial participation of caveolin-1. In contrast, a transmembrane protein, the cystic fibrosis transmembrane conductance regulator, exhibited transient anchorage that occurred without deliberately enhanced cross-linking; moreover, it was only slightly inhibited by cholesterol depletion or SFK inhibition and depended completely on the interaction of its PDZ-binding domain with the cytoskeletal adaptor EBP50. We propose that cross-linked GPIAPs become transiently anchored via a cholesterol-dependent SFK-regulatable linkage between a transmembrane cluster sensor and the cytoskeleton.

Introduction

The general signaling mechanisms by which the cross-linking of membrane determinants induces linkage to the cytoskeleton is a long-standing issue dating back to the original patching and capping observations (Raff et al., 1970) and the ideas of Singer (Singer, 1977; Holifield et al., 1990). More recently, such attachments have assumed clearer physiological and pathological importance. For example, receptor-induced dimerization (Lidke et al., 2005) causes retrograde transport off the filopodia to distal sites for further processing. Bead-induced clustering of integrins and cell adhesion molecules causes retrograde transport of these molecules away from the leading edge, and considerable effort has been devoted to the manner by which different sized ligand-coated beads induce clusters of cell adhesion molecules to link to the retrograde actin flow (Felsenfeld et al., 1996; Suter et al., 1998; Suter and Forscher, 2001). After binding to membrane receptors, viral particles are eventually associated with the cytoskeleton in different ways (Pelkmans et al., 2002; Ewers et al., 2005). T cell activation, which is initiated by ligation, is mediated by T cell receptor–containing microclusters that reorganize in an actin-dependent manner (Yokosuka et al., 2005).

Even lipids and glycosyl-phosphatidylinositol–anchored proteins (GPIAPs), when cross-linked, undergo patching and capping (Schroit and Pagano, 1981; Holifield et al., 1990), and GPIAPs can signal across the plasma membrane. The binding of antibody to several GPIAPs was shown early on to induce an association with Src family kinases (SFKs; Stefanova et al., 1991). Cross-linking the GPIAP Thy-1 on T lymphocytes results in mitogenesis (Kroczek et al., 1986; Zhang et al., 1992). Group B coxsackieviruses begin the process of infection of epithelial cells by binding to and clustering the GPIAP coreceptor decay-accelerating factor on the apical surface (Coyne and Bergelson, 2006). Transmembrane signaling has been speculated to occur in nanodomains such as lipid rafts when clusters are induced via

Correspondence to Ken Jacobson: frap@med.unc.edu

Abbreviations used in this paper: Cbp, C-terminal Src kinase–binding protein; CFTR, cystic fibrosis transmembrane conductance regulator; GPIAP, glycosyl-phosphatidylinositol–anchored protein; RAT, relative anchorage time; RCT, relative confinement time; SFK, Src family kinase; SPT, single-particle tracking; SV40, Simian virus 40; TCZ, transient confinement zone.

The online version of this article contains supplemental material.

The Journal of Cell Biology, Vol. 175, No. 1, October 9, 2006 169–178
http://www.jcb.org/cgi/doi/10.1083/jcb.200512116

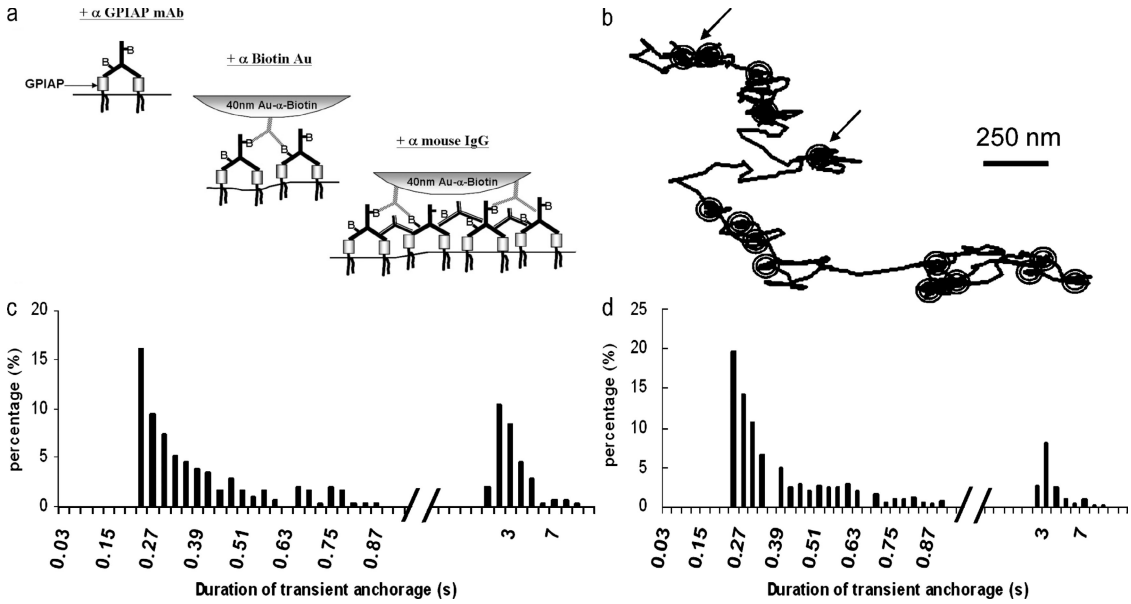

Figure 1. **Maximal cross-linking scheme that produces transient anchorage.** (a) After incubating cells with biotinylated mouse primary antibodies recognizing specific GPIAPs (top), antibiotin gold particles are added on the cell membrane to form bonds with the primary antibodies (middle). Finally, tertiary polyclonal antibodies that bind to mouse IgG are added to further cross-link the GPIAPs (bottom). (b) During SPT, short periods with zero displacement were observed (arrows indicate representative transient anchorage events). (c) The periods of transient anchorage for maximally cross-linked CD73 on IMR 90 cells varied from several hundred milliseconds to >10 s and are bimodally distributed. (d) Preassembled complexes also showed a similar bimodal distribution of transient anchorage durations.

receptor ligation and cross-linking (Simons and Toomre, 2000), and such signaling may serve to link the cluster to the cytoskeleton (Kusumi et al., 2004). However, the precise mechanisms of how GPIAPs signal and link to the cytoskeleton remain to be elucidated. This issue remains central in the study of the functionality of membrane microdomains (Kusumi et al., 2004).

In this study, we use a novel feature of single-particle tracking (SPT) trajectories as an assay to begin a dissection of how the linkage of certain GPIAPs and transmembrane proteins to the membrane-associated cytoskeleton may be regulated. SPT has been used to study membrane heterogeneity on various time and distance scales. Using video rate SPT, gold particles bound to membrane lipids and proteins were found temporarily corralled in transient confinement zones (TCZs; Simson et al., 1995; Sheets et al., 1997; Dietrich et al., 2002; Chen et al., 2004). With much higher time resolution, gold particles that bound to lipids and GPIAPs undergo compartmentalized hop diffusion on the millisecond time scale (Kusumi et al., 2005). Most previous experiments were aimed at producing pauci- or univalent gold to minimize the number of membrane molecules bound to gold so as to minimize artifacts caused by cross-linking membrane molecules (Murase et al., 2004). In contrast, in this study, we deliberately used the gold particle to form clusters of GPIAPs, mimicking the clusters formed under physiological conditions. The size of clusters associated with gold particles is much smaller than the size of clusters that were seen by immunostaining in previous studies (i.e., patches), which may represent ~1,000 molecules (Holifield et al., 1990; Mayor et al., 1994). This protocol produced a unique nanoscale signature in the SPT trajectories, termed transient anchorage, that depends on SFKs, PI3 kinase, cholesterol, and caveolin-1. In some respects, our study confirms and extends the findings of Suzuki et al. (2004) using the GPIAP CD59. A transmembrane protein, the cystic fibrosis transmembrane conductance regulator (CFTR), also exhibits transient anchorage that strictly depends on its C-terminal PDZ-binding domain, but it is regulated differently than the GPIAP anchorage.

Results

Transient anchorage

Mild cross-linking of membrane molecules by paucivalent gold is most likely the reason for transient confinement (Kusumi et al., 2004; Murase et al., 2004). However, in our hands, this type of transient confinement was not sensitive to inhibitors of SFKs (unpublished data), which is in contrast to results reported by Kusumi et al. (2004). We reasoned that perhaps our level of cross-linking was insufficient to induce the involvement of SFKs. Therefore, we used three different layers of cross-linking antibodies (Fig. 1 a) to collect the GPIAPs of interest together under and proximate to a single gold particle. The trajectories of these clusters on the cell membrane reveal how signal transduction influences the lateral motion of GPIAPs that are sufficiently cross-linked.

We chose to investigate two GPIAPs, Thy-1 and CD73 (a 5′ exonucleotidase), both of which are endogenously expressed. The trajectories of both molecules exhibited a surprising feature: a considerable number of temporary anchorage events could be observed in the video record (Fig. 1 b and Video 1, available at http://jcb.org/cgi/content/full/jcb.200512116/DC1). To automatically identify the transient anchorage, a detection program was developed. Transient anchorage, in which particles stop (no displacement within experimental error) transiently, is

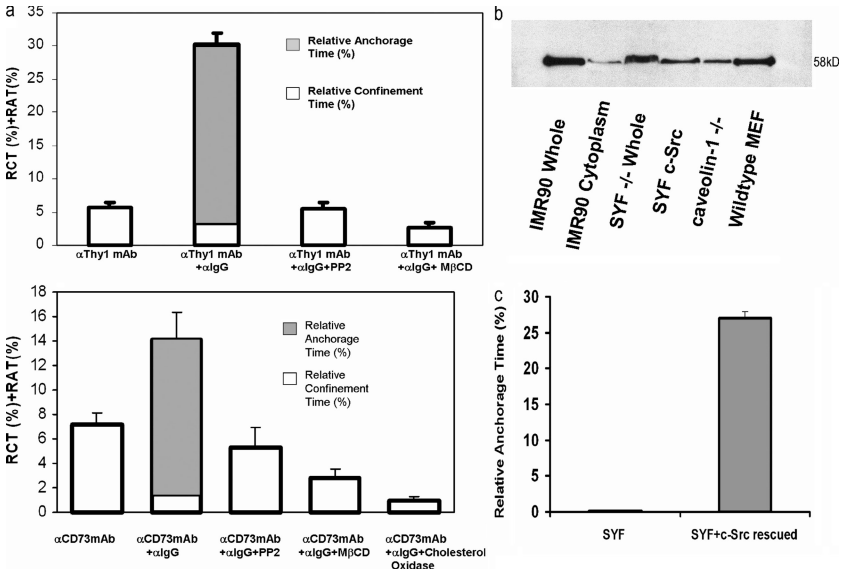

Figure 2. **Both SFK inhibition and cholesterol depletion suppressed transient anchorage.** (a) C3H expressing Thy-1 (top) and IMR 90 cells expressing CD73 (bottom) were treated with PP2 (n = 79 for Thy-1 and n = 79 for CD73 where n is the number of trajectories analyzed) or cholesterol-removing agents, mβCD (n = 100 for Thy-1 and n = 70 for CD73), and/or cholesterol oxidase (n = 67 for CD73) before maximal cross-linking. SPT with maximal cross-linking was the positive control (n = 90 for Thy-1 and n = 88 for CD73). SPT without maximal cross-linking (without tertiary antibody addition) was the negative control (n = 69 for Thy-1 and n = 85 for CD73). Error bars indicate the SEM. (b) Western blotting was performed to check the expression of CD73 and whether the anti–human CD73 antibody can detect CD73 on the human and mouse cell lines used in this study. MEF, mouse embryonic fibroblast. (c) SFKs are required for the transient anchorage of CD73. SFK-deficient cells (n = 65) did not demonstrate transient anchorage upon maximal cross-linking, but transient anchorage can be rescued by the transfection of c-Src (n = 80) into the deficient cell line. (a and c) The results were collected over three to five independent experiments.

distinguished from transient confinement, in which single particles still diffuse but in a slower and confined manner (Dietrich et al., 2002). The periods of transient anchorage varied from several hundred milliseconds to >10 s as shown in an example from cross-linked CD73 on IMR 90 cells and are bimodally distributed (Fig. 1 c). The longer anchorage times are directly visible in the video record. Fig. 2 a shows how the total relative confinement, combining both TCZs and transient anchorage for both Thy-1 (top) and CD73 (bottom), was increased by the maximal cross-linking protocol up to seven times compared with the control (left), in which the tertiary cross-linking antibody was not applied. Note that despite different definitions of transient anchorage and transient confinement, transient anchorage points sometimes overlapped with TCZs. Therefore, to avoid the overestimation of relative confinement time (RCT) + relative anchorage time (RAT), the time segments in the trajectory in which transient anchorage was detected were removed, and the trajectory was concatenated. This operation resulted in a decreased RCT in trajectories in which transient anchorage was detected.

Transient anchorage only occurred after the addition of the tertiary antibodies (Fig. 1 a, bottom right) and showed titration behavior (Table I) so that there was an optimum concentration at a dilution of ∼1:100 with the final concentration of 20 μg/ml. The dependence of transient anchorage on the concentration of tertiary antibody suggests that a critical size and/or number of cross-linked GPIAPs is required for transient anchorage (Harder and Simons, 1999). Having too many tertiary antibodies will result in a competition for the available binding sites offered by the primary antibodies; this will lead to monovalent binding of the tertiary antibody with diminished cross-linking and transient anchorage.

Transient anchorage also occurs with preassembled complexes: estimate of cluster size

The number of molecules cross-linked in one cluster is important for constructing a detailed mechanism of transient anchorage. In the maximal cross-linking protocol, primary antibodies are first bound to specific GPIAPs (Fig. 1); antibiotin gold is then added, decorating the surface at a very low concentration. Finally, tertiary antibody is added. Under these conditions, it is difficult to estimate the size of the cluster aggregated under one particle. In addition, the possibility of distal patches of cross-linked GPIAPs globally affecting the behavior of the gold particles cannot be excluded.

Therefore, we preassembled gold particle–antibody complexes to test whether transient anchorage would still occur. These complexes contain antibiotin gold with biotinylated anti–mouse IgG antibodies and anti–Thy-1 antibodies. An approximation to the number of primary antibodies bound to each gold particle in the preassembled complexes was made by estimating the contact area between the gold particle and cell membrane (see Gold conjugation to cells, procedure II). The estimate suggests that the maximal number of gold-bound Thy-1 molecules is likely to be <135 and is probably much less. These preassembled complexes exhibited transient anchorage, although the RAT was somewhat reduced (20%) compared with the original protocol (28%; Fig. S2 b, available at http://www.jcb.org/cgi/content/full/jcb.200512116/DC1). The bimodal distribution of

Table I. **Dependence of CD73 transient anchorage on dilution of the tertiary antibody**

Dilution ratio[a]	Total confinement[b]	RCT	RAT
	%	%	%
1:2,000	7.0 ± 1.0	7.0 ± 1.0	Not detected
1:1,000	10.8 ± 1.7	10.8 ± 1.7	Not detected
1:200	15.1 ± 2.7	7.2 ± 0.1	12.2 ± 1.6
1:100	36.8 ± 2.4	15.0 ± 1.7	31.4 ± 2.2
1:50	14.5 ± 2.0	10.7 ± 1.7	11.5 ± 1.1

Data are given as the mean ± SEM.
[a]Concentration of stock solution = 2 mg/ml.
[b]To avoid overestimation, the total confinement is obtained by adding RCT and RAT and subtracting the overlapping time in which transient anchorage and TCZs both occurred.

anchorage times was similar to that seen in the maximal cross-linking SPT experiments (Fig. 1 d). Thus, a cluster of <135 GPIAPs is sufficient to induce transient anchorage.

Regulation of transient anchorage

Role of cholesterol. To examine the role of cholesterol, which is found enriched in detergent-resistant membranes and is hypothesized to be an essential component of rafts, in transient anchorage, we performed cholesterol depletion before the maximal cross-linking. SPT trajectories obtained from treated cells were compared with the control. Transient anchorage was not detected in cells depleted of cholesterol by M CD (Thy-1 and CD73; Fig. 2 a, top and bottom, respectively) or removed by cholesterol oxidase (CD73; Fig. 2 a, bottom). Both Thy-1 and CD73 showed reduced transient confinement upon cholesterol depletion, which is consistent with previous studies (Sheets et al., 1997; Dietrich et al., 2001).

Role of SFKs. GPIAPs such as CD59 and Thy-1 are found to couple with SFKs, which are distributed in the inner leaflet of the cell membrane, to effect signal transduction (Stefanova et al., 1991). It has also been shown that filamentous actin accumulates under patches of GPIAPs (Harder and Simons, 1999). The actin enrichment requires the activities of Fyn and Lck kinases (Harder and Simons, 1999), both of which belong to the Src family. A plausible hypothesis is that SFKs mediate the process of tethering the cross-linked GPIAP clusters to the membrane-associated cytoskeleton. Indeed, a form of transient confinement with the GPIAP CD59 has been shown to be mediated by Lck (Kusumi, 2004). Thus, we treated cells with the specific SFK inhibitor PP2 before the cross-linking. Transient anchorage was completely suppressed for both GPIAPs tested (Fig. 2 a), indicating that SFKs are critical for stabilization of the clusters. However, transient confinement was not substantially affected. Because transient anchorage occurs with preassembled particles, the possibility that global activation of SFKs by the maximal cross-linking protocol is responsible for transient anchorage is excluded.

We used the Src, Yes, and Fyn (SYF) triple knockout mouse fibroblast cells to confirm these results. Our anti–human CD73 antibody bound to CD73 on SYF cells, and Src rescued SYF cells as assessed by immunostaining (not depicted) and Western blots from these cells (Fig. 2 b). SYF defective cells showed no transient anchorage and reduced confinement similar to PP2-treated cells. However, transient anchorage was restored in Src-rescued SYF cells (Fig. 2 c). Thus, SFK activity is crucial for the transient anchorage phenotype.

Role of PI3 kinase. Phosphoinositides PIP_2 and PIP_3 copatch with cross-linked raft components (Janes et al., 1999). It has also been shown that signaling via cross-linked GPIAP and choleratoxin-labeled cholesterol-containing clusters on the cell surface is blocked by both tyrosine kinase and PI3 kinase inhibition (Krauss and Altevogt, 1999), suggesting the involvement of PIP_2 and PIP_3 in signaling events induced by cross-linking. In addition, PIP_2 and PIP_3 found in inner leaflet microdomains are also involved in cytoskeletal regulation (Janmey and Lindberg, 2004). These findings suggest that changing the balance of PIP_2 and PIP_3 by inhibiting PI3 kinase might affect transient anchorage. To test this possibility, before SPT experiments, IMR 90 cells were incubated with the PI3 kinase inhibitor LY294004 for 15 min. Compared with control cells, PI3 kinase–inhibited cells exhibited more than a threefold greater transient anchorage (Fig. 3 a). However, the proportion of the longer anchorage times was drastically reduced (compare Fig. 3 b with Fig. 1 c). Moreover, inspection revealed that half of the trajectories (23/47) exhibited bidirectional movements in the PI3 kinase–inhibited cells with excursions up to several micrometers (Fig. 3 c).

Role of caveolin. Because cholesterol depletion also disrupts the structure of caveolae, which has been demonstrated by electron microscopy (Parpal et al., 2001; Dreja et al., 2002),

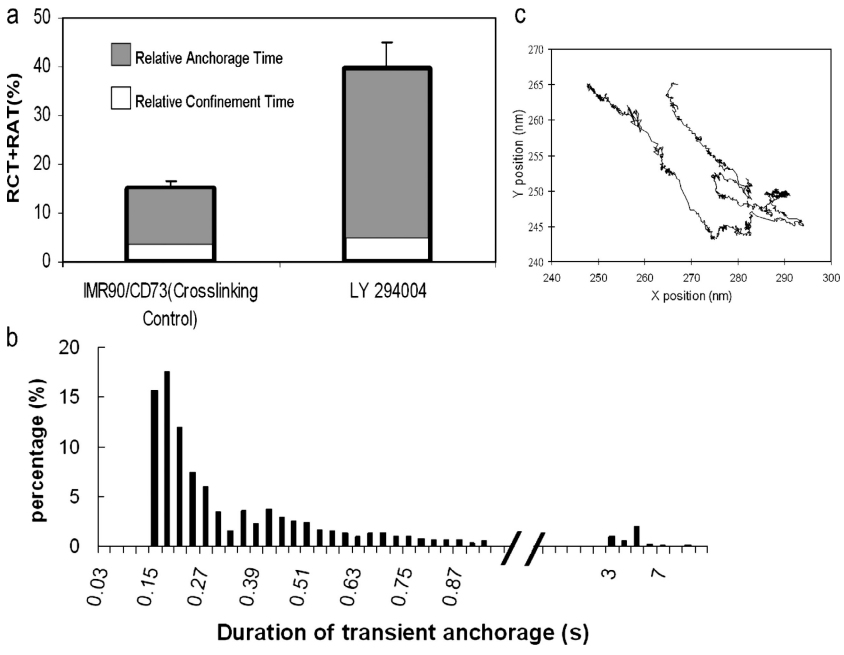

Figure 3. **Effects of PI3 inhibition on transient anchorage.** (a) PI3 kinase inhibition induced more transient anchorage upon maximal cross-linking (n = 117) compared with the control cells (n = 120). The results were collected over three to four independent experiments. Error bars indicate the SEM. (b) Compared with Fig. 1 c, longer anchorage times were largely abolished in PI3 kinase–inhibited cells. (c) A portion of single particles after PI3 inhibition exhibited bidirectional movements, as shown by this representative trajectory.

a plausible possibility was that caveolae and caveolin might have a role in transient anchorage. Supporting this possibility, patches of cross-linked GPIAPs were found associated with caveolae (Mayor et al., 1994). By coimmunostaining of caveolin-1 and maximally cross-linked Thy-1 on C3H cells, we confirmed that cross-linked glycosyl-phosphatidylinositol–anchored Thy-1 partially colocalizes with caveolin-1 (Fig. 4, c and d). Similar results were obtained for CD73 and caveolin-1 in IMR 90 cells (Fig. 4, a and b). In contrast, if cells were prefixed and subjected to maximal cross-linking, minimal colocalization was observed (unpublished data).To test the involvement of caveolin-1 in the transient anchorage phenotype, we used caveolin-1 knockout mouse embryonic fibroblasts. The expression of caveolin-1 was checked in knockout and control wild-type embryonic fibroblasts by immunostaining and confirmed the absence of caveolin-1 on the cell surface of the knockout cells but not the wild type (unpublished data). Also, both caveolin-1 wild-type cells and knockout cells express CD73 (Fig. 2 b). As shown in Fig. 4 c, the RAT was reduced from ~45% in wild-type cells to ~15% in caveolin-1 knockout cells. After PP2 treatment to inhibit SFKs, the RAT was reduced to <5% in both knockout and wild-type cells. A similar effect was observed when cholesterol depleted from both cell types. The result suggests that caveolin-1 contributes to the transient anchorage, although apparently other mechanisms are also involved, as indicated by the persistence of transient anchorage that is PP2 inhibitable in caveolin-1 knockout cells.

Transient anchorage exhibited by a transmembrane protein is regulated in a different manner

To further test whether the critical role of SFKs in the transient anchorage of GPIAPs is related to phosphorylation-enabled cytoskeletal association of clustered GPIAPs, we examined the diffusion behavior of a transmembrane protein, the CFTR. The C-terminal cytoplasmic domain of CFTR associates with the actin cytoskeleton via Na^+/H^+ exchanger regulatory factor PDZ proteins (EBP50 and E3KARP) and ezrin (Short et al., 1998; Sun et al., 2000; Raghuram et al., 2003). If transient cytoskeletal association is the cause of transient anchorage and cross-linking is necessary to recruit SFKs for clustered GPIAPs to be linked to the cytoskeleton, CFTR might be expected to demonstrate transient anchorage in a cross-linking and SFK-independent manner. Furthermore, if cholesterol involvement in the transient anchorage of GPIAPs is required because SFKs can only be recruited under the clusters through cholesterol-mediated nanodomains, CFTR might also be expected to demonstrate transient anchorage independent of cholesterol.

CFTR tagged with an extracellular HA epitope was expressed in C3H cells and labeled with biotinylated anti-HA antibodies and antibiotin antibody–conjugated gold. We found that CFTR displayed transient anchorage in the absence of tertiary cross-linking antibody (Fig. 5). Upon PP2 or cholesterol depletion treatment, gold-conjugated HA-CFTR demonstrated only a modest reduction in RAT (Fig. 5), whereas both Thy-1 and CD73 showed a marked decrement in RAT after the same treatments (Fig. 2 a). Also, deletion of the PDZ-binding domain in CFTR, the Δ4 mutant (Gentzsch et al., 2004), caused transient anchorage to be almost completely eliminated (Fig. 5), indicating that Na^+/H^+ exchanger regulatory factor (EBP50) PDZ proteins and ezrin provide the key linkage to the cytoskeleton that is required for the transient anchorage of CFTR to occur. Thus, GPIAPs exhibit a much more marked dependence of transient anchorage on SFK and cholesterol than does transmembrane CFTR. This suggests a mechanism by which cross-linked GPIAPs could exploit (via a cholesterol-mediated nanodomain followed by SFK regulation) the normal linkages of transmembrane proteins to the cytoskeleton (see Discussion).

Discussion

Robust transient anchorage was observed with the maximal cross-linking protocol. The preassembled complexes clustering 135 or fewer Thy-1 GPIAPs are shown to be sufficient to trigger transient anchorage comparable with the clusters formed by maximal cross-linking. Cholesterol is essential for gold particle–bound clusters to be transiently anchored on the cell surface,

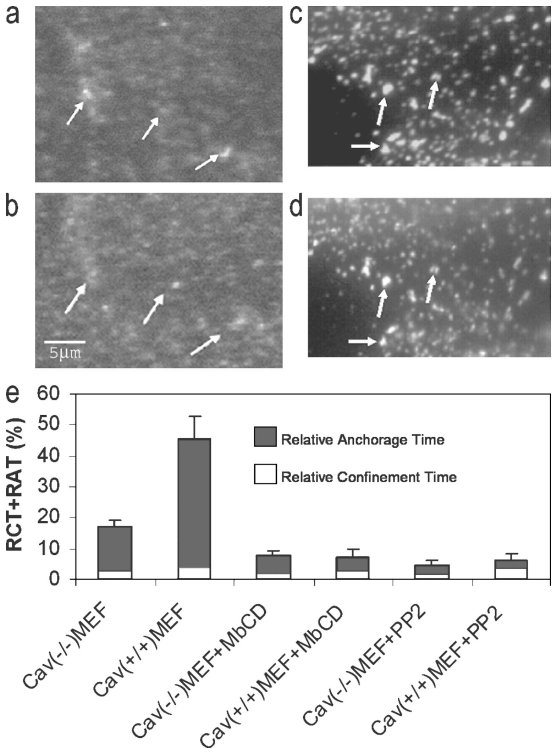

Figure 4. **Caveolae participated in transient anchorage.** (a and b) Partial colocalization between CD73 (a) and caveolin-1 (b) was seen on IMR 90 cells after maximal cross-linking. (c and d) Partial colocalization between Thy-1 (c) and caveolin-1 (d) was seen on C3H cells after maximal cross-linking. The specificity of primary and secondary antibodies used here has been examined by the manufacturers and they do not cross react. (a–d) Arrows show representative regions of colocalization. (e) In caveolin-1–deficient mouse embryonic cells (n = 92), transient anchorage of Thy-1was reduced to about one third compared with wild-type parental cells (n = 100). Transient anchorage could be suppressed by SFK inhibition and cholesterol depletion in both cell lines (n = 70 for caveolin$^{-/-}$ + MβCD; n = 72 for caveolin$^{+/+}$ + MβCD; n = 88 for caveolin$^{-/-}$ + PP2; and n = 75 for caveolin$^{+/+}$ + PP2). The results were collected over three to five independent experiments. Error bars indicate the SEM. MEF, mouse embryonic fibroblast.

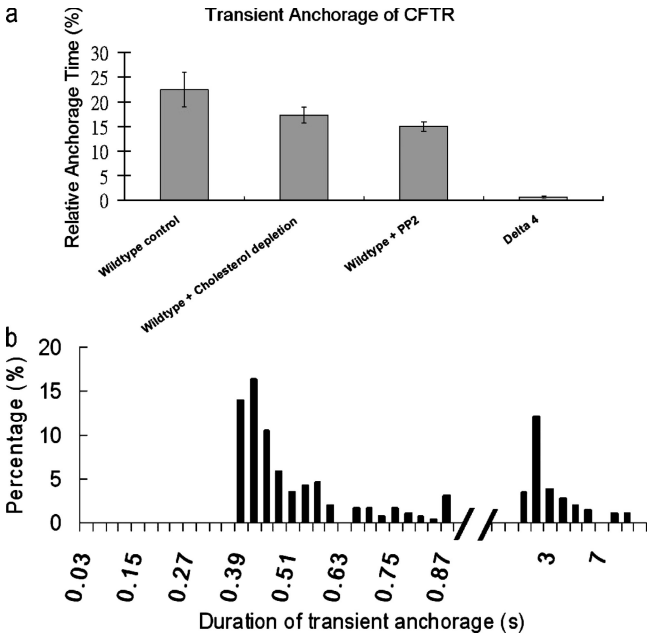

Figure 5. **CFTR demonstrated transient anchorage independent of maximal cross-linking, SFK activities, and cholesterol presence.** (a) CFTR tagged with an extracellular HA epitope was expressed in C3H cells and labeled with biotinylated anti-HA antibodies and antibiotin antibody–conjugated gold for SPT. CFTR displayed transient anchorage in the absence of tertiary cross-linking antibody ($n = 74$). SFK inhibition (by PP2; $n = 60$) or cholesterol depletion (by MβCD; $n = 60$) only slightly reduced the transient anchorage, whereas deletion of the PDZ-binding domain in CFTR (Δ4 mutant; $n = 65$) caused transient anchorage to be almost completely eliminated. Error bars indicate the SEM. (b) CFTR demonstrated a similar bimodal distribution of transient anchorage durations compared with the maximal linked CD73 in Fig. 2 c.

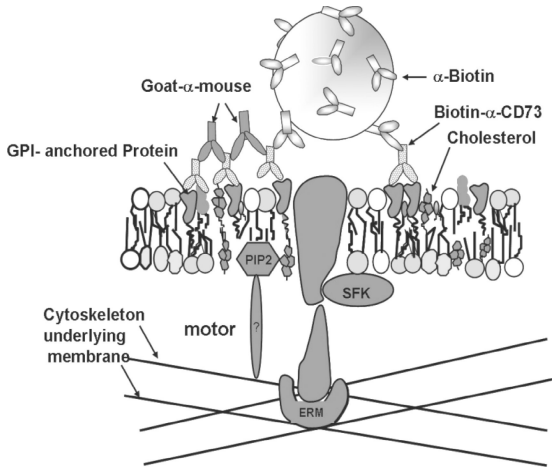

Figure 6. **Transient anchorage hypothesis.** Cross-linking causes nanodomains to form on both the inner and outer leaflet, with a transmembrane protein bridging the two leaflets to transduce the signal. When an activated SFK randomly partitions into such a nanodomain, phosphorylation by the SFK causes a resident molecule, possibly the transmembrane protein, to attach to the actin cytoskeleton indirectly through other linker proteins. The attachment results in a transient anchorage until the SFK becomes deactivated and a recruited phosphatase dephosphorylates the linking resident molecule in the nanodomain (see Discussion for details). ERM, ezrin/radixin/moesin proteins; PIP_2, phosphatidyl-inositol bisphosphate; SFK, Src family kinase.

suggesting that a cholesterol-dependent nanodomain is formed under maximally cross-linked gold particles. The cross-linking–triggered signaling events involve SFK cascades, PI3 kinase, and caveolin-1. What molecular mechanisms might account for this phenomenon? The broad outlines of how different modes of transient anchorage might occur can be gleaned from recent reviews. Simons and Toomre (2000) suggested that the cross-linking of receptors might be a key to effecting signal transduction by either altering partitioning into existing raft domains or bringing smaller rafts together. Kusumi et al. (2004) suggested that one mode of coupling clustered GPIAPs may involve an unspecified transmembrane protein and recruitment of small inner leaflet rafts containing lipid-linked signaling molecules to the site of the cluster raft on the outer leaflet.

To focus future experiments, we propose a somewhat more specific working hypothesis (Fig. 6) using these ideas as a starting point. In this model, cross-linking induces cholesterol-dependent nanodomains (cluster rafts) to form on both the inner and outer leaflet. Such clusters would include key transmembrane proteins bridging the inner and outer leaflets so that signals could be transmitted across the membrane in discrete locations. These proteins would be included from the outset and/or incorporated after collision of the cluster with the transmembrane protein. Whether initial anchoring is assisted by oligomerization-induced trapping (Kusumi et al., 2005) is an open issue. When an activated SFK randomly partitions into such a nanodomain on the inner leaflet, phosphorylation by SFK induces a resident transmembrane molecule to attach to the actin cytoskeleton through adaptor proteins. The attachment results in a transient anchorage event that continues until the SFK is deactivated and a recruited phosphatase dephosphorylates the resident linking molecule.

Specific molecular players can be accommodated by this generic hypothesis. A novel SFK substrate, C-terminal Src kinase–binding protein (Cbp; or PAG), was identified recently as a transmembrane protein-binding partner for C-terminal Src kinase, a kinase that regulates SFKs by phosphorylation at their C-terminal regulatory site (Matsuoka et al., 2004). There is also evidence indicating that Thy-1 is associated with Cbp (Durrheim et al., 2001). Furthermore, after phosphorylation by proximate SFKs, Cbp binds the ERM (ezrin/radixin/moesin)-binding protein (EBP50) via its PDZ domain and, thus, associates with the cytoskeleton through ERM proteins (Itoh et al., 2002). Therefore, Cbp is a plausible candidate for the transmembrane protein component of the hypothesis. Indeed, we have obtained results that are at least consistent with the transient anchorage of GPIAPs proceeding via the EBP50-ERM-actin cytoskeleton linkage: an EBP50-binding transmembrane protein, CFTR, exhibits transient anchorage without using the maximal cross-linking protocol, and removal of the C-terminal PDZ-binding domain of CFTR, which binds EBP50, in the Δ4 mutant (Gentzsch et al., 2004) abrogates transient anchorage (Fig. 5). Therefore, our hypothesis suggests that there is a common mode of cytoskeletal binding for both CFTR and GPIAPs (via EBP50-ezrin) but two different ways to couple to these adaptors, either directly (CFTR) or indirectly (GPIAP) via the formation of nanodomains and SFK regulation. Indeed, a regulatable ezrin linkage to Cbp was recently hypothesized to link rafts

containing the B cell receptor to the lymphocyte cytoskeleton (Gupta et al., 2006).

Previous studies have shown that caveolin-1 deficiency diminishes both the number of caveolae (Drab et al., 2001) and caveolin-2 expression (Razani et al., 2001). Therefore, the diminution of transient anchorage in caveolin-1$^{-/-}$ cells is consistent with some of it occurring in caveolar structures. Alternatively or additionally, other cellular functions of caveolin-1 and -2 may be associated with transient anchorage. In their studies of the mobility of Simian virus 40 (SV40) on the cell surface before and just after its entry into the cell, Damm et al. (2005) also found a partial dependence on caveolin-1. Their findings can be compared and contrasted with our study. After diffusing, SV40 often stops as opposed to being transiently anchored as a prelude to internalization via caveolin-1–dependent or –independent pathways. However, only the caveolin-1–independent internalization pathway of SV40 requires tyrosine kinase activity and cholesterol.

In our study, transient anchorage does not exclusively depend on caveolin-1, suggesting at least two pathways to anchorage, but both pathways depended on cholesterol and SFK. Damm et al. (2005) also used SPT to study the diffusion behavior of mouse polyoma viruslike particles (which are 45 nm in diameter and similar to the size of gold particles) bound to live cell membranes and found cholesterol-dependent but SFK-independent confinement (Ewers et al., 2005). Viruslike particles exhibited confined diffusion in small zones 30–60 nm in diameter, which differs from transient anchorage in the fact that neither SFKs nor caveolin is required for confinement. Confinement requires the cross-linking of viral receptor (ganglioside), which promotes linkage to the actin cytoskeleton in an as yet undefined way. In general, based on the extensive study of viral interactions with the cell membrane, it could be anticipated that multiple modes of transient anchorage would exist (Marsh and Helenius, 2006).

Unexpectedly, inhibition of the conversion of PIP_2 into PIP_3 by PI3 kinase enhances transient anchorage and induces directional motion in a substantial fraction of trajectories. It is possible that PIP_2 may preferentially partition into the inner leaflet microdomains induced by the cross-linked clusters of GPIAPs, and transient anchorage might then be formed via PIP_2 to adaptor proteins that are associated with the actin cytoskeleton underneath the cell membrane, such as the ERM family proteins (Fievet et al., 2004). The bidirectional movements observed in some of the trajectories suggests that PIP_2 clusters that participate in transient anchorage might also bind to motor proteins through their FERM or pleckstrin homology domains, thus contributing to the directed transport of cross-linked clusters by walking along cytoskeletal filaments. Binding between clustered PIP_2 and motor proteins also provides a possible explanation for the disappearance of longer stopping periods because the motor proteins are active most of the time and might be expected to move the cluster directionally with short pauses (Kural et al., 2005).

Collectively, our data suggests that the transient anchorage phenotype may be regulated in different ways depending on the biological context. Moreover, the transient anchorage assay presented here should be valuable in defining precise linkages to the cytoskeleton and how they are regulated.

Materials and methods

Cells

C3H 10T1/2 mouse fibroblasts (American Type Culture Collection [ATCC]) and IMR 90 human fibroblasts were maintained in basal medium Eagle and DME, respectively, and both were supplemented with 10% FBS, 100 units/ml penicillin, and 100 μg/ml streptomycin. 2–4 d before an SPT experiment, fibroblasts were plated onto sterile 22 × 22-mm coverslips (glass) that were placed into 35-mm petri dishes at an appropriate cell density that yielded single cells for SPT measurements. Cells were depleted of cholesterol by treatment with 5 mM MβCD (Sigma-Aldrich) at 37°C for 30 min in unsupplemented medium or with 0.5 units of cholesterol oxidase (C8273; Sigma-Aldrich) at 37°C for 1 h in complete medium, respectively. The Src$^{-/-}$, Yes$^{-/-}$, and Fyn$^{-/-}$ mouse embryonic cell line (SYF; ATCC) and the SYF cell line with restored c-Src expression by the retroviral vector pLXSH (SYF^{+}; ATCC) were used to examine the effect of SFKs on transient anchorage. The caveolin-1–deficient mouse embryonic cell line (caveolin-1$^{-/-}$) and its wild-type parental cell line, which were gifts from M. Schwartz (University of Virginia, Charlottesville, VA), were used for experiments investigating the role of caveolin-1 in transient anchorage. HA-tagged CFTR protein was expressed in C3H cells by LipofectAMINE (Invitrogen) transfection.

Gold conjugation to cells

Procedure I. Antibiotin mouse IgG gold (BBInternational) was dissolved in Ham's F-12 nutrition mixture (Life Technologies/Invitrogen) supplemented with 25 mM Hepes and 15% serum (HHS), sedimented by centrifugation for 15 min at 11,000 *g* at 4°C, and resuspended in HHS. Cells on the coverslips were first incubated with biotinylated primary antibodies (1.5 mg/ml monoclonal mouse anti–Thy-1 antibody [clone 19EX5] or 0.15 mg/ml monoclonal mouse anti–human CD73 antibody [clone AD2; a gift from L. Thompson, Oklahoma Medical Research Foundation, Oklahoma City, OK]) for 10 min and were washed three times with 1 ml HH (HHS without serum). Then, the coverslip was mounted to form an open chamber on the slide with spacers on two parallel edges of the coverslip. 100 μl of the solution containing antibiotin gold (4.5×10^9 particles/ml) was injected into the chamber and incubated with cells for 10 min at 37°C. Unbound gold particles were removed by washing with 100 μl HH. 100 μl of the solution containing tertiary antibodies (0.02 mg/ml goat anti–mouse IgG; Zymed Laboratories) for the purpose of maximal cross-linking was injected into the chamber at this time if required. A final washing step with 100 μl of injected HHS was performed to remove unbound gold. For SPT of CFTR, 0.1 mg/ml biotinylated mouse anti-HA antibody (clone 16B12; Covance) was used as the primary antibody followed by the addition of antibiotin gold. SPT was then performed without the addition of cross-linking tertiary antibodies. For all experiments, after the gold particle incubations, the sample chamber was sealed with wax and mounted on the microscope. Particle trajectories were recorded for the following 30 min at 37°C and were maintained by an air curtain incubator.

Procedure II (preassembled complexes). Gold particles conjugated with antibodies specific to GPIAPs of interest were assembled before addition to the cells. Preassembled complexes (Fig. S2 a) were made by mixing 20 μl antibiotin gold (4.5×10^{11} particles/ml), 2 μl biotinylated goat anti–mouse IgG antibodies (2 mg/ml), and 20 μl mouse anti–Thy-1 antibodies (15.5 mg/ml) in HHS solution with a final volume of 2 ml. The preassembled complexes were then spun down, resuspended, and added to the cell membrane for SPT experiments as described in the previous paragraph for procedure I. On the basis of the number of antibiotin conjugated to gold (150 antibodies/particle) as specified by the manufacturer (BBInternational), the biotinylated goat anti–mouse IgG antibodies (2.6×10^{-11} mol) added were in 10-fold excess over the antibiotin antibodies coated on gold, and the mouse anti–Thy-1 antibodies (10^{-9} mol) added were in 40-fold excess over the goat anti–mouse IgG antibodies.

Immunofluorescence

Colocalization of cross-linked GPIAPs with caveolin-1. Cross-linking of GPIAPs was accomplished by incubating cells with biotinylated primary monoclonal antibodies followed by antibiotin gold (BBInternational) and AlexaFluor488 polyclonal goat anti–mouse IgG antibody (Invitrogen) as in procedure I in the Gold conjugation to cells section. Cells were fixed with a mixture of 2% PFA and 2.5% glutaraldehyde for 10 min, washed three

times with PBS, and permeabilized with 1% NP-40. Rabbit anti–mouse caveolin-1 antibody (Santa Cruz Biotechnology, Inc.) and Texas red–labeled goat anti–rabbit IgG antibody (Oncogene Research Products) were used to stain the caveolin-1 inside the cell. After extensive washing in PBS, cells on the coverslips were mounted on the slide with FluorSave reagent (Calbiochem) and observed using a fluorescence microscope (IX-81; Olympus) with a 100× objective. The fluorescent images of fixed samples were taken by a dual-mode cooled CCD camera (C4880; Hamamatsu) with MetaMorph image acquisition software (Molecular Devices) at room temperature. As a negative control in immunostaining, cells were prefixed in the 2% PFA and 2.5% glutaraldehyde mixture, after which the maximal cross-linking protocol was used; under such conditions, clustering of the GPIAPs would not be expected.

Time-lapse gold imaging for SPT

Computer-enhanced video microscopy, which was described previously (Lee et al., 1991), was used to image colloidal gold bound to the plasma membrane of fibroblast cells. In brief, the cell lamella with bound gold was imaged in brightfield mode and recorded with a video camera (Newvicon; Hamamatsu). After real-time background subtraction and contrast enhancement with an image processing unit (Argus 20; Hamamatsu), video frames were recorded in time-lapse mode (1,800 frames with 30 frames/s) on the hard disk of a computer (O2; Silicon Graphics). Recorded videos were analyzed by the commercial software package ISee (Inovision Corp.), which identifies relative changes of gold particle positions on the cell lamella with a precision of ±20 nm. All trajectories were visually inspected to ensure the correct tracking of gold particles.

Data analysis

Trajectories of gold particles obtained from SPT videos were analyzed for both transient confinement and transient anchorage. The detection for TCZs was performed as described previously (Simson et al., 1995). Transient anchorage detection software was designed to detect regions of trajectories where no displacement within experimental error occurred, as defined by all aspects of measurement stability. By recording videos of gold particles firmly glued on coverslips using nail polish and then detecting particle centroids over the time recorded, it was determined that 95% of centroids fell within ±25 nm along both the x and y axis (Fig. S1, available at http://www.jcb.org/cgi/content/full/jcb.200512116/DC1). A program was developed to recognize fragments from a trajectory as potential transient anchorage events when the displacement in successive frames was <25 nm in both the x and y dimensions. To qualify as transient anchorage, this condition must have persisted for more than four video frames (132 ms). Note that transient anchorage differs from immobilization, in which the particle does not move during the experimental observation time of a particular cell. To further characterize transient anchorage, we defined the RAT as the sum of durations in which a single particle is transiently anchored/total time of trajectory. To avoid the overestimation of total confinement given that transient anchorage sometimes overlaps with TCZs, transient anchorage segments were removed from the trajectories, and the remaining trajectory fragments were concatenated before TCZ detection.

Estimation of the maximum number of GPIAPs bound to preassembled complexes

We calculated this estimate using the following considerations. Gold particles almost appear to float on the membrane and can diffuse rapidly. This suggests that they are not nearly enveloped by the plasma membrane. The degree to which they can bend the membrane around them will determine the maximum number of membrane antigens the preassembled complex can bind. The bending modulus determines how facilely the membrane can be molded. However, the bending modulus will depend on the length scale examined. For example, if the particle is over an actin or spectrin filament, bending will not be as easy as if the particle is in the region between filaments. The maximum bending may be estimated in the following way. Let us say the compartment dimension of the cytoskeleton meshwork underlying the membrane is ~100 nm. As shown in Fig. S2 a, taking the thickness of a single layer of antibodies to be 10 nm (Kienberger et al., 2004), the overall preassembled complex diameter would maximally be 100 nm. For the sake of argument, say each membrane (bilayer plus peripheral proteins) is ~10 nm thick, so the gold particle complex in which a membrane partially wraps it has a radius of 60 nm. The furthest the membrane-wrapped particle could sink between adjacent filaments (Fig. S2 a) would result in the membrane covering the gold–antibody complex with a coverage area (CA), given by the equation

$$CA = 2\pi r^2 \left[1 - \cos\alpha\right] \quad (1),$$

where α represents the half angle corresponding to the contact area and r represents the radius of the whole complex (Fig. S2 a). For the geometrical situation depicted in Fig. S2 a, $\alpha \approx 56°$. Assuming each binding site is saturated by the antibodies added in the next layer, the maximal number of surface Thy-1 bound to the particle is calculated as

$$\text{Max. \# bound Thy-1} = 600 \times 2 \times 2\pi r^2 \left[1 - \cos\alpha\right] / 4\pi r^2 \quad (2).$$

In equation 2, the number of available anti–Thy-1 antibodies on the particle was multiplied by two because of the bivalency of antibodies (total number bound = 600). Given that r = 60 nm and $1 - \cos\alpha \approx 0.45$, the maximum number of bound Thy-1 was calculated as being ≤135. Considering the possible inactivation by partial denaturation of antibiotin antibodies during the coating process on gold particles, the steric and orientation considerations preventing antibody binding, and whether the particle actually sinks to the extent postulated in calculation, the actual number of Thy-1 bound to the preassembled complexes could be much less.

In equilibrium, the free energy gained from the antibody–antigen interaction should be greater than or equal to the energy required to bend the membrane to conform the membrane to the particle (E_{bend}). To bend an area of the membrane with an effective radius of curvature of 60 nm will require an energy given by

$$E_{bend} = \text{Area} \times kc / \left[2 \times (r^2)\right] \quad (3),$$

where kc represents the bending modulus of the cell membrane, r is the radius of curvature, and the area is given by the calculation in equation 1 (Sackmann, 1994). The local bending modulus will most likely lie somewhere between that for a bilayer, in which $kc \approx 2\ 8\ k_BT$ at 37°C (Waugh et al., 1992), and that for the red cell membrane, in which $kc \approx 23 k_BT$ (Evans, 1980). This leads to E_{bend} values ranging from 40 k_BT, if pure bilayer intervened between the cytoskeletal filaments (Sako and Kusumi, 1995), to 33 k_BT, if the red cell membrane modulus is more appropriate. The energy released from antibody–antigen bond formation ranges from 11 to 22 k_BT at 37°C, corresponding to K_a values from 10^5 and 10^{10} M^{-1} (Van Regenmortel, 1998). Therefore, the free energy released from only four or fewer antibody–antigen bonds would be sufficient to bend the membrane to the extent required by the aforementioned extreme model.

While this paper was being reviewed, a study concluded that so much energy is gained from ligand–receptor bonds that the plasma membrane would completely envelope a 100-nm–diameter HIV particle (Sun and Wirtz, 2006). Our calculation assumes that the complete envelopment of a coated 40-nm gold particle would be frustrated by the presence of immediately subjacent cytoskeletal filaments. Then, between transient anchorage points, gold particles also diffuse rapidly, which seems unlikely if they were completely enveloped.

Image acquisition descriptions

In Fig. 4 (a–d), we used a microscope (IX-81; Olympus) with a 100× NA 1.25 oil immersion objective (Olympus). FluorSave reagent (Calbiochem) was used as the imaging medium, and AlexaFluor488 (Fig. 4, a and c) and Texas red (Fig. 4, b and d) were used as the fluorochromes. Images were captured with a dual-mode cooled CCD camera (C4880; Hamamatsu) and MetaMorph image acquisition software (Molecular Devices). Photoshop (Adobe) was used to crop the whole cell images into small fractions.

Online supplemental material

Fig. S1 shows determination positional noise in the SPT system. Fig. S2 shows that preassembled complexes bound to ≤135 GPIAPs still demonstrate transient anchorage. Video 1 shows that the gold-bound cross-linked Thy-1 cluster is diffusing on the C3H membrane with transient anchorage. Online supplemental material is available at http://www.jcb.org/cgi/content/full/jcb.200512116/DC1.

We thank G. Schuetz for helpful discussions.

This work was supported by the National Institutes of Health (grant GM 41402 to K. Jacobson) and Cystic Fibrosis Foundation (grant to S.L. Milgram).

Submitted: 21 December 2005
Accepted: 31 August 2006

References

Chen, Y., B. Yang, and K. Jacobson. 2004. Transient confinement zones: a type of lipid raft? *Lipids*. 39:1115–1119.

Coyne, C.B., and J.M. Bergelson. 2006. Virus-induced Abl and Fyn kinase signals permit coxsackievirus entry through epithelial tight junctions. *Cell*. 124:119–131.

Damm, E.M., L. Pelkmans, J. Kartenbeck, A. Mezzacasa, T. Kurzchalia, and A. Helenius. 2005. Clathrin- and caveolin-1-independent endocytosis: entry of simian virus 40 into cells devoid of caveolae. *J. Cell Biol.* 168:477–488.

Dietrich, C., Z.N. Volovyk, M. Levi, N.L. Thompson, and K. Jacobson. 2001. Partitioning of Thy-1, GM1, and cross-linked phospholipid analogs into lipid rafts reconstituted in supported model membrane monolayers. *Proc. Natl. Acad. Sci. USA*. 98:10642–10647.

Dietrich, C., B. Yang, T. Fujiwara, A. Kusumi, and K. Jacobson. 2002. Relationship of lipid rafts to transient confinement zones detected by single particle tracking. *Biophys. J.* 82:274–284.

Drab, M., P. Verkade, M. Elger, M. Kasper, M. Lohn, B. Lauterbach, J. Menne, C. Lindschau, F. Mende, F.C. Luft, et al. 2001. Loss of caveolae, vascular dysfunction, and pulmonary defects in Caveolin-1 gene-disrupted mice. *Science*. 293:2449–2452.

Dreja, K., M. Voldstedlund, J. Vinten, J. Tranum-Jensen, P. Hellstrand, and K. Sward. 2002. Cholesterol depletion disrupts caveolae and differentially impairs agonist-induced arterial contraction. *Arterioscler. Thromb. Vasc. Biol.* 22:1267–1272.

Durrheim, G.A., D. Garnett, K.M. Dennehy, and A.D. Beyers. 2001. Thy-1 associated pp85–90 is a potential docking site for SH2 domain-containing signal transduction molecules. *Cell Biol. Int.* 25:33–42.

Evans, E.A. 1980. Minimum energy analysis of membrane deformation applied to pipet aspiration and surface adhesion of red blood cells. *Biophys. J.* 30:265–284.

Ewers, H., A.E. Smith, I.F. Sbalzarini, H. Lilie, P. Koumoutsakos, and A. Helenius. 2005. Single-particle tracking of murine polyoma virus-like particles on live cells and artificial membranes. *Proc. Natl. Acad. Sci. USA*. 102:15110–15115.

Felsenfeld, D.P., D. Choquet, and M.P. Sheetz. 1996. Ligand binding regulates the directed movement of beta1 integrins on fibroblasts. *Nature*. 383:438–440.

Fievet, B.T., A. Gautreau, C. Roy, L. Del Maestro, P. Mangeat, D. Louvard, and M. Arpin. 2004. Phosphoinositide binding and phosphorylation act sequentially in the activation mechanism of ezrin. *J. Cell Biol.* 164:653–659.

Gentzsch, M., X.B. Chang, L. Cui, Y. Wu, V.V. Ozols, A. Choudhury, R.E. Pagano, and J.R. Riordan. 2004. Endocytic trafficking routes of wild type and DeltaF508 cystic fibrosis transmembrane conductance regulator. *Mol. Biol. Cell*. 15:2684–2696.

Gupta, N., B. Wollscheid, J.D. Watts, B. Scheer, R. Aebersold, and A.L. DeFranco. 2006. Quantitative proteomic analysis of B cell lipid rafts reveals that ezrin regulates antigen receptor-mediated lipid raft dynamics. *Nat. Immunol.* 7:625–633.

Harder, T., and K. Simons. 1999. Clusters of glycolipid and glycosylphosphatidylinositol-anchored proteins in lymphoid cells: accumulation of actin regulated by local tyrosine phosphorylation. *Eur. J. Immunol.* 29:556–562.

Holifield, B.F., A. Ishihara, and K. Jacobson. 1990. Comparative behavior of membrane protein-antibody complexes on motile fibroblasts: implications for a mechanism of capping. *J. Cell Biol.* 111:2499–2512.

Itoh, K., M. Sakakibara, S. Yamasaki, A. Takeuchi, H. Arase, M. Miyazaki, N. Nakajima, M. Okada, and T. Saito. 2002. Cutting edge: negative regulation of immune synapse formation by anchoring lipid raft to cytoskeleton through Cbp-EBP50-ERM assembly. *J. Immunol.* 168:541–544.

Janes, P.W., S.C. Ley, and A.I. Magee. 1999. Aggregation of lipid rafts accompanies signaling via the T cell antigen receptor. *J. Cell Biol.* 147:447–461.

Janmey, P.A., and U. Lindberg. 2004. Cytoskeletal regulation: rich in lipids. *Nat. Rev. Mol. Cell Biol.* 5:658–666.

Kienberger, F., H. Mueller, V. Pastushenko, and P. Hinterdorfer. 2004. Following single antibody binding to purple membranes in real time. *EMBO Rep.* 5:579–583.

Krauss, K., and P. Altevogt. 1999. Integrin leukocyte function-associated antigen-1-mediated cell binding can be activated by clustering of membrane rafts. *J. Biol. Chem.* 274:36921–36927.

Kroczek, R.A., K.C. Gunter, B. Seligmann, and E.M. Shevach. 1986. Induction of T cell activation by monoclonal anti-Thy-1 antibodies. *J. Immunol.* 136:4379–4384.

Kural, C., H. Kim, S. Syed, G. Goshima, V.I. Gelfand, and P.R. Selvin. 2005. Kinesin and dynein move a peroxisome in vivo: a tug-of-war or coordinated movement? *Science*. 308:1469–1472.

Kusumi, A. 2004. Single molecule imaging of raft dynamics and raft-based signal transduction in living cells. *Biophysical Society Meeting*. 7 pp.

Kusumi, A., I. Koyama-Honda, and K. Suzuki. 2004. Molecular dynamics and interactions for creation of stimulation-induced stabilized rafts from small unstable steady-state rafts. *Traffic*. 5:213–230.

Kusumi, A., H. Ike, C. Nakada, K. Murase, and T. Fujiwara. 2005. Single-molecule tracking of membrane molecules: plasma membrane compartmentalization and dynamic assembly of raft-philic signaling molecules. *Semin. Immunol.* 17:3–21.

Lee, G.M., A. Ishihara, and K.A. Jacobson. 1991. Direct observation of brownian motion of lipids in a membrane. *Proc. Natl. Acad. Sci. USA*. 88:6274–6278.

Lidke, D.S., K.A. Lidke, B. Rieger, T.M. Jovin, and D.J. Arndt-Jovin. 2005. Reaching out for signals: filopodia sense EGF and respond by directed retrograde transport of activated receptors. *J. Cell Biol.* 170:619–626.

Marsh, M., and A. Helenius. 2006. Virus entry: open sesame. *Cell*. 124:729–740.

Matsuoka, H., S. Nada, and M. Okada. 2004. Mechanism of Csk-mediated down-regulation of Src family tyrosine kinases in epidermal growth factor signaling. *J. Biol. Chem.* 279:5975–5983.

Mayor, S., K.G. Rothberg, and F.R. Maxfield. 1994. Sequestration of GPI-anchored proteins in caveolae triggered by cross-linking. *Science*. 264:1948–1951.

Murase, K., T. Fujiwara, Y. Umemura, K. Suzuki, R. Iino, H. Yamashita, M. Saito, H. Murakoshi, K. Ritchie, and A. Kusumi. 2004. Ultrafine membrane compartments for molecular diffusion as revealed by single molecule techniques. *Biophys. J.* 86:4075–4093.

Parpal, S., M. Karlsson, H. Thorn, and P. Stralfors. 2001. Cholesterol depletion disrupts caveolae and insulin receptor signaling for metabolic control via insulin receptor substrate-1, but not for mitogen-activated protein kinase control. *J. Biol. Chem.* 276:9670–9678.

Pelkmans, L., D. Puntener, and A. Helenius. 2002. Local actin polymerization and dynamin recruitment in SV40-induced internalization of caveolae. *Science*. 296:535–539.

Raff, M.C., M. Sternberg, and R.B. Taylor. 1970. Immunoglobulin determinants on the surface of mouse lymphoid cells. *Nature*. 225:553–554.

Raghuram, V., H. Hormuth, and J.K. Foskett. 2003. A kinase-regulated mechanism controls CFTR channel gating by disrupting bivalent PDZ domain interactions. *Proc. Natl. Acad. Sci. USA*. 100:9620–9625.

Razani, B., J.A. Engelman, X.B. Wang, W. Schubert, X.L. Zhang, C.B. Marks, F. Macaluso, R.G. Russell, M. Li, R.G. Pestell, et al. 2001. Caveolin-1 null mice are viable but show evidence of hyperproliferative and vascular abnormalities. *J. Biol. Chem.* 276:38121–38138.

Sackmann, E. 1994. The seventh Datta Lecture. Membrane bending energy concept of vesicle- and cell-shapes and shape-transitions. *FEBS Letters*. 346:3–16.

Sako, Y., and A. Kusumi. 1995. Barriers for lateral diffusion of transferrin receptor in the plasma membrane as characterized by receptor dragging by laser tweezers: fence versus tether. *J. Cell Biol.* 129:1559–1574.

Schroit, A.J., and R.E. Pagano. 1981. Capping of a phospholipid analog in the plasma membrane of lymphocytes. *Cell*. 23:105–112.

Sheets, E.D., G.M. Lee, R. Simson, and K. Jacobson. 1997. Transient confinement of a glycosylphosphatidylinositol-anchored protein in the plasma membrane. *Biochemistry*. 36:12449–12458.

Short, D.B., K.W. Trotter, D. Reczek, S.M. Kreda, A. Bretscher, R.C. Boucher, M.J. Stutts, and S.L. Milgram. 1998. An apical PDZ protein anchors the cystic fibrosis transmembrane conductance regulator to the cytoskeleton. *J. Biol. Chem.* 273:19797–19801.

Simons, K., and D. Toomre. 2000. Lipid rafts and signal transduction. *Nat. Rev. Mol. Cell Biol.* 1:31–39.

Simson, R., E.D. Sheets, and K. Jacobson. 1995. Detection of temporary lateral confinement of membrane proteins using single-particle tracking analysis. *Biophys. J.* 69:989–993.

Singer, S.J. 1977. Thermodynamics, the structure of integral membrane proteins, and transport. *J. Supramol. Struct.* 6:313–323.

Stefanova, I., V. Horejsi, I.J. Ansotegui, W. Knapp, and H. Stockinger. 1991. GPI-anchored cell-surface molecules complexed to protein tyrosine kinases. *Science*. 254:1016–1019.

Sun, F., M.J. Hug, C.M. Lewarchik, C.H. Yun, N.A. Bradbury, and R.A. Frizzell. 2000. E3KARP mediates the association of ezrin and protein kinase A with the cystic fibrosis transmembrane conductance regulator in airway cells. *J. Biol. Chem.* 275:29539–29546.

Sun, S.X., and D. Wirtz. 2006. Mechanics of enveloped virus entry into host cells. *Biophys. J.* 90:L10–L12.

Suter, D.M., and P. Forscher. 2001. Transmission of growth cone traction force through apCAM-cytoskeletal linkages is regulated by Src family tyrosine kinase activity. *J. Cell Biol.* 155:427–438.

Suter, D.M., L.D. Errante, V. Belotserkovsky, and P. Forscher. 1998. The Ig superfamily cell adhesion molecule, apCAM, mediates growth cone steering by substrate-cytoskeletal coupling. *J. Cell Biol.* 141:227–240.

Suzuki, K., T. Fujiwara, K. Ritchie, F. Sanematsu, H. Hirano, M. Edidin, and A. Kusumi. 2004. Rapid diffusion of putative raft molecules indicative of the absence of large stable rafts in the resting-state cell membrane. *Biophysical Society Annual Meeting.* Abstr. 348.

Van Regenmortel, M.H. 1998. Thermodynamic parameters in immunoassay. *Clin. Chem. Lab. Med.* 36:353–354.

Waugh, R.E., J. Song, S. Svetina, and B. Zeks. 1992. Local and nonlocal curvature elasticity in bilayer membranes by tether formation from lecithin vesicles. *Biophys. J.* 61:974–982.

Yokosuka, T., K. Sakata-Sogawa, W. Kobayashi, M. Hiroshima, A. Hashimoto-Tane, M. Tokunaga, M.L. Dustin, and T. Saito. 2005. Newly generated T cell receptor microclusters initiate and sustain T cell activation by recruitment of Zap70 and SLP-76. *Nat. Immunol*. 6:1253–1262.

Zhang, F., W.G. Schmidt, Y. Hou, A.F. Williams, and K. Jacobson. 1992. Spontaneous incorporation of the glycosyl-phosphatidylinositol-linked protein Thy-1 into cell membranes. *Proc. Natl. Acad. Sci. USA*. 89:5231–5235.